water

MDPI

Article

Piezo-Photocatalytic Degradation of Pharmaceuticals in Water Using Calcined Natural Sphalerite

Svetlana Popova [1], Victoria Tazetdinova [1,2], Erzhena Pavlova [2], Galina Matafonova [1,*] and Valeriy Batoev [1]

[1] Laboratory of Engineering Ecology, Baikal Institute of Nature Management SB RAS, 670047 Ulan-Ude, Russia
[2] Chemistry Faculty, Buryat State University, 670000 Ulan-Ude, Russia
* Correspondence: ngal@binm.ru

Abstract: This study is the first to report the high performance of calcined natural sphalerite as a heterogeneous catalyst (Catalyst) in the piezo- and photocatalytic degradation of pharmaceuticals (bezafibrate and ceftriaxone) using high-frequency ultrasound (US, 1.7 MHz) and ultraviolet-light-emitting diodes (LED, 365 nm). The kinetic comparison showed that piezo-photocatalysis (LED + US + Catalyst) was more efficient than photocatalysis (LED + Catalyst) for degrading both contaminants in deionized water as well as in surface river water at natural pH (7.9). Despite reducing degradation rates (~1.7 times) in river water due to the scavenging effect of its constituents, ceftriaxone and bezafibrate were degraded by 77% and 48% after 1 h of exposure, respectively. Adding H_2O_2 increased the corresponding pseudo-first-order rate constants, and the complete degradation of ceftriaxone was achieved. However, the contribution of ultrasound at a given intensity was hidden, which resulted in a similar performance of piezo-photocatalysis and photocatalysis for treating river water. No pronounced synergy between the piezo- and photocatalytic processes was observed in the experimental conditions used. Nevertheless, the H_2O_2-assisted piezo-photocatalysis using high-frequency US, LED, and natural catalysts can be considered a novel and effective strategy for eliminating pharmaceuticals from real water without pH adjustment.

Keywords: natural sphalerite; ZnO; 365 nm LED; 1.7 MHz ultrasound; pharmaceuticals; degradation; piezo-photocatalysis

check for updates

Citation: Popova, S.; Tazetdinova, V.; Pavlova, E.; Matafonova, G.; Batoev, V. Piezo-Photocatalytic Degradation of Pharmaceuticals in Water Using Calcined Natural Sphalerite. *Water* **2023**, *15*, 3092. https://doi.org/10.3390/w15173092

Academic Editor: Chengmei Liao

Received: 5 July 2023
Revised: 22 August 2023
Accepted: 24 August 2023
Published: 29 August 2023

Copyright: © 2023 by the authors. Licensee MDPI, Basel, Switzerland. This article is an open access article distributed under the terms and conditions of the Creative Commons Attribution (CC BY) license (https://creativecommons.org/licenses/by/4.0/).

1. Introduction

Rapid industrialization and the increasing global consumption of drugs have led to the contamination of aquatic ecosystems with pharmaceuticals and their metabolites. WHO identifies pharmaceuticals as emerging contaminants, which generate public concern about drinking water safety [1]. To date, the pollution of natural surface water with pharmaceuticals (especially antibiotics) has become a global problem that poses a great risk to environmental and human health [2]. The development of green and cost-effective technologies for the elimination of pharmaceuticals from water and wastewater is crucial for reducing their discharge and adverse effects and moving towards the United Nations' Sustainable Development Goal 6.3 (to improve water quality by reducing pollution, eliminating dumping, and minimizing the release of hazardous chemicals, materials, and untreated wastewater).

Over the past few years, piezo-photocatalysis has emerged as a new approach for environmental remediation, including the degradation of organic contaminants in water [3–5]. It uses piezoelectric semiconductor materials, which exhibit both piezoelectric and photocatalytic properties under mechanical and light exposure in water. The mechanical energy, in turn, comes from ultrasonic vibration, vortex-induced shearing force, or physical bending [6]. Briefly, the internal electric fields, which are induced via the piezoelectric effect, improve the separation of photogenerated electron–hole pairs to enhance the generation of reactive oxygen species (ROS, primarily •OH) upon reaction with O_2 and H_2O and,

finally, the catalytic performance. Recent reviews showed that in most piezo-photocatalytic processes, the piezoelectric effect was driven by ultrasound [3,4].

ZnO is a bio-friendly piezoelectric semiconductor with a non-centrosymmetric structure [7]. To date, ZnO and various composites on its basis have been fabricated and successfully examined for the piezo-photocatalytic degradation of organic contaminants, mainly dyes [3,4,6,8,9]. Pharmaceuticals as target contaminants have received less attention; however, in recent years, there has been growing interest in their degradation by piezo-photocatalysis with ZnO-based materials (Table 1).

Table 1. Summary of recent literature on the piezo-photocatalytic degradation of pharmaceuticals using fabricated ZnO-based piezo-photocatalysts.

Catalyst	Pharmaceutical	Ultrasonic Frequency	Light Source/Wavelength	Performance	Reference
ZnO/CuS nanorods, 400 mg/L	Tetracycline, 30 mg/L	not reported	Xenon lamp	85.28% for 60 min vs. 73.89% (photocatalysis) and 40.51% (piezo-catalysis).	[10]
Ca-ZnO nanoparticles	Tetracycline, 10 mg/L	40 kHz	White LED, >400 nm	≥99% mineralization in 90 min.	[11]
Cu/ZnO, 0.1 g/L Ni-ZnO, 0.15 g/L	Cefixime	40 kHz	Tungsten lamp (visible)	45.7% (Cu-ZnO), 42.2% (Ni-ZnO) in 30 min. H_2O_2 increased the efficiency.	[12]
AgI/ZnO, 200 mg/L	Tetracycline, 10 mg/L	40 kHz	Xenon lamp, >400 nm	94.7% in 120 min.	[13]
Pure ZnO, 0.1 g/L	Diclofenac, 25 mg/L	20 kHz	UVA halide lamp, 320–400 nm	70% degradation of in 360 min.	[14]
MgO/ZnO/graphene nanocomposite, 0.8 g/L	Sulfamethoxazole, 55 mg/L	24 kHz	UVA LED	Complete degradation in 120 min.	[15]
Pure ZnO, 0.6 g/L	Penicillin G and cefixime, 100 mg/L	40 kHz	LP mercury lamp, 254 nm	94.2% for penicillin G and 84.2% for cefixime. Biodegradability increased.	[16]
Pure ZnO, 200–400 mg/L	Cephalexin, 50–100 mg/L	40 kHz	LP mercury lamp, 254 nm	Degradation under optimal conditions in 120 min.	[17]
Pure ZnO, 0.4 g/L	Salicylic acid	35 kHz	UVB lamp	Complete degradation within 200 min. H_2O_2 enhanced degradation.	[18]

As shown in Table 1, low-frequency ultrasound below 100 kHz (typically 20–40 kHz) was used in previous studies. Meanwhile, high-frequency ultrasound appears to be more efficient than low-frequency ultrasound in view of enhanced ROS generation [19–21]. Laurenti et al. (2020) [22] demonstrated that 1 MHz was efficient for the piezo- and photocatalytic degradation of Rhodamine-ß dye (66% in 60 min) using ZnO:Sb films. As such, high-frequency ultrasound above the 100 kHz and MHz range is emerging as a promising strategy for boosting the performance of piezo-catalysts.

While fabricated catalysts, including ZnO-based (nano)composites, offer high performance, they are high-cost products and may be toxic for aquatic biota, making it difficult to scale up their application in water treatment. In this regard, naturally occurring semiconductor minerals, which are abundant in the Earth's crust, represent an attractive alternative to fabricated catalysts due to their easy accessibility, low cost, and non-toxicity. To date,

natural photoactive minerals have gained considerable attention as cost-effective catalysts for environmental remediation, mainly for water disinfection [23–29]. There have also been a few studies on the photocatalytic degradation of dyes using natural sphalerite [30,31] and wolframite [32].

Another emerging research area lies in the development of photocatalysts on the basis of natural minerals, which could make them less expensive to manufacture. For instance, recent studies reported the fabrication of TiO_2 anchored in natural pyrite for photocatalytic water disinfection [33], as well as Fe_3O_4 natural iron ore/calcium alginate beads [34] and sea sediment@400/ZnO [35] for the degradation of dyes by photo-Fenton and piezo-photocatalysis with 24 kHz, respectively.

To the best of our knowledge, natural minerals have not been used for piezo-photocatalytic degradation of organic contaminants using high-frequency ultrasound (above 100 kHz). Our previous work showed the catalytic activity of calcined natural sphalerite, composed primarily of ZnO, in matrix-free (deionized) water under simultaneous exposure to high-frequency ultrasonic and UVA radiation [36]. However, the effect of co-existing components of a real aqueous matrix remains unexplored. This is the first study that aims to evaluate the photocatalytic and piezo-photocatalytic performance of calcined natural sphalerite towards the degradation of pharmaceuticals in deionized and natural water. Testing real water is crucial for assessing the feasibility of the novel method for practical application. The lipid-lowering drug bezafibrate (BZF) and ß-lactam cephalosporin antibiotic ceftriaxone (CTX) were selected as target compounds. High-frequency ultrasound (1.7 MHz) and ultraviolet-light-emitting diodes (UV LEDs, 365 nm) were used as drivers of the piezo-photocatalytic process. The degradation kinetics in the absence and presence of H_2O_2 were studied, and •OH exposure was estimated. A potential synergistic effect of piezo-photocatalysis was examined and compared with literature data.

2. Materials and Methods

2.1. Reagents

Bezafibrate ($C_{19}H_{20}ClNO_4$, 99%) and ceftriaxone sodium ($C_{18}H_{16}N_8Na_2O_7S_3$, 99%) were products of Sigma-Aldrich (St. Louis, MO, USA). Hydrogen peroxide (33%) (Lega LLC, Dzerzhinsk, Russia), titanium oxysulfate (Alfa Aesar, Karlsruhe, Germany), orthophosphoric and acetic acid (JSC Khimreaktivsnab, Ufa, Russia) were used as received. Sulfuric acid was supplied by Sigma Tek LLC (Moscow, Russia). HPLC-grade acetonitrile was purchased from Cryochrom (St. Petersburg, Russia). Deionized water (18.2 MΩ·cm) was produced by a Simplicity®UV system (Millipore, Molsheim, France).

2.2. Natural Catalyst

The catalyst was natural sphalerite from the Dovatka ore deposit in the Buryatia Republic (Siberia, Russia). Its characteristics and the preparation process were described in detail in our previous study [36]. Briefly, the ore sample was crushed on a ball mill, ground, and sieved to obtain a powder with particle sizes below 75 μm (Figure 1).

The main elements of natural sphalerite were Zn (61.8%) and S (34%) [36]. Since the highest photocatalytic activity was previously observed after calcination at 900 °C for 5 h, the catalyst was calcined under the same conditions for the present study (muffle furnace SNOL-1150, AB Umega, Ukmergė, Lithuania). ZnO was a major phase (E_g = 3.2 eV), which was responsible for the photocatalytic activity of calcined natural sphalerite upon excitation at 365 nm.

2.3. Water Matrices

Deionized and natural water were used as matrices in degradation experiments. Natural surface water was collected from the Selenga River, the main tributary of Lake Baikal (Siberia, Russia). The samples were filtered immediately after delivery (0.45 μm NC, Ikeme, Guangzhou, China) and stored at 4 °C prior to experiments. The general water quality parameters are given in Table 2.

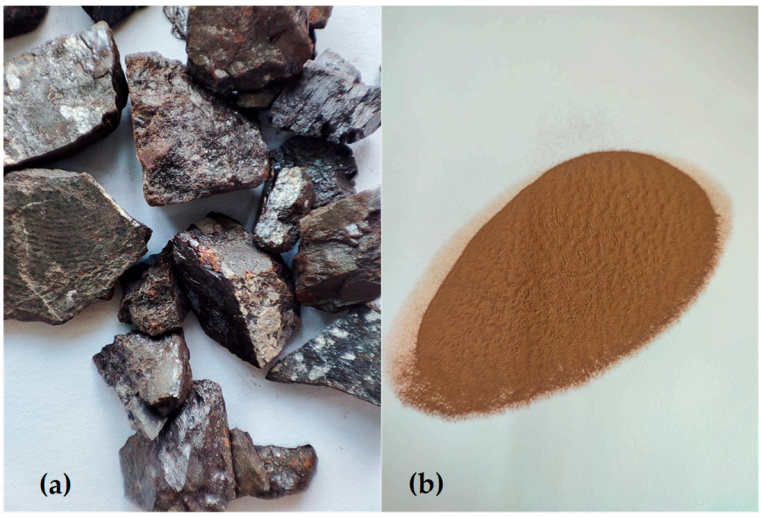

Figure 1. Samples of ore (**a**) and prepared (**b**) natural sphalerite.

Table 2. General quality parameters of river water for experiments.

Parameter	Value
pH	7.9 ± 0.2
Conductivity, mS/cm	235.0 ± 0.1
DOC [1], mg/L	2.09 ± 0.25
Bicarbonate, mg/L	131.2 ± 15.7
Carbonate, mg/L	<6.0
Nitrite, mg/L	<0.1
Nitrate, mg/L	2.95 ± 0.38
Ammonium, mg/L	0.12 ± 0.04
Total iron, mg/L	0.10 ± 0.02
Chloride, mg/L	1.98 ± 0.26
Phosphate, mg/L	<0.1
Sulfate, mg/L	15.63 ± 2.03
COD [2], mg/L	14.40 ± 3.04

[1] Dissolved organic carbon. [2] Chemical oxygen demand.

2.4. Experimental Procedure

Degradation experiments were sequentially conducted in deionized water and river water using a batch piezo-photoreactor (Figure 2), which was previously described in detail [36].

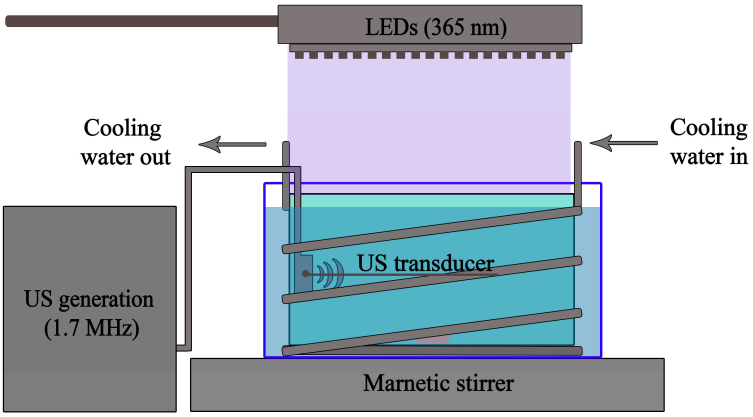

Figure 2. A diagram of piezo-photoreactor with 365 nm LEDs and 1.7 MHz ultrasound.

Briefly, it comprises a thermostated glass vessel, a UV LED matrix (365 nm), and an orthogonally positioned piezo-electric transducer (US, 1.7 MHz). In a typical experiment, 100 mL of water matrix, contaminated with 20 μM BZF or CFX, was irradiated at unadjusted pH in the absence and presence of freshly ground 1 g/L catalyst and 1 mM H_2O_2 (Table 3).

Table 3. The series of experiments in this study.

1st Series	2nd Series
LED only	LED + H_2O_2
US only	US + H_2O_2
LED + US	LED + US + H_2O_2
US + Catalyst	US + Catalyst + H_2O_2
LED + Catalyst	LED + Catalyst + H_2O_2
LED + US + Catalyst	LED + US + Catalyst + H_2O_2

The effect of pH was examined after the pre-acidification of river water with 1 N H_2SO_4 solution. The samples were periodically collected over 60 min of treatment, centrifuged at 4000 rpm for 5 min (C2006, Centurion Scientific, Chichester, West Sussex, UK), filtered through 0.25 μm PTFE membrane filters (CJSC Vladisart, Vladimir, Russia) to remove the catalyst particles, and analyzed for the residual concentration of the target contaminant. Recycling tests were conducted for the photocatalytic (LED + Catalyst) degradation of BZF in deionized water. After the first run, the catalyst was washed with water, centrifuged and dried at 100 °C overnight before next cycle [37,38].

•OH exposure was evaluated with scavenging experiments, which were performed in all examined systems using *p*-chlorobenzoic acid (*p*CBA) as a probe compound ($k_{p\mathrm{CBA},\bullet\mathrm{OH}} = 5 \times 10^9\ \mathrm{M^{-1}\ s^{-1}}$ [39]). The steady-state concentration of hydroxyl radicals ($[\bullet\mathrm{OH}]_{ss}$) was calculated from the observed pseudo-first-order rate constant of *p*CBA decay (k_{obs}, $\mathrm{s^{-1}}$) (1, 2):

$$-\frac{d[p\mathrm{CBA}]}{dt} = k_{p\mathrm{CBA},\bullet\mathrm{OH}} \cdot [p\mathrm{CBA}][\bullet\mathrm{OH}]_{ss} \quad (1)$$

$$[\bullet\mathrm{OH}]_{ss} = \frac{k_{obs}}{k_{p\mathrm{CBA},\ \bullet\mathrm{OH}}} \quad (2)$$

2.5. Analysis

The concentrations of BZF and CTX were determined by HPLC using an Agilent 1260 Infinity chromatograph with a UV detector and Zorbax SB-C18 column (4.6 × 150 mm, 5 μm) (Santa Clara, CA, USA). The eluent was a mixture of acetonitrile with 0.1% orthophosphoric acid (30:70) for CTX (0.3 mL/min) and acetic acid (60:40) for BZF (0.5 mL/min). CTX and BZF were detected at 270 and 228 nm, respectively. The kinetics of *p*CBA degradation were also monitored using HPLC by eluting with a mixture of methanol and 1% acetic acid (70:30) and detecting at 230 nm. Each data point on the degradation plots represents the mean value (±SD) from 3 to 5 replicates.

DOC in river water was measured with a TOC-L CSN analyzer (Shimadzu, Kyoto, Japan). pH measurements were performed using a Pocket Meter Multi 3510 IDS (WTW, Weilheim, Germany). Hydrochemical analysis of river water samples was carried out following the standard methods, which are listed in the Environmental Normative Federal Documents (Federal Center of Analysis and Assessment of Technogenic Exposure, Moscow, Russia) and equivalent to the Standard Methods [40]. H_2O_2 consumption was determined by a modified colorimetric method with titanium oxysulfate [41]. The method is based on the reaction of titanyl ions with H_2O_2 under acidic conditions with a formation of yellow-colored pertitanic acid. The absorbance was measured at 420 nm (ε = 532 $\mathrm{M^{-1}\ cm^{-1}}$) using a Shimadzu UV-1800 spectrophotometer (Shimadzu, Kyoto, Japan). The statistical treatment of the data was carried out with the Statistica 10.0 software program.

3. Results and Discussion

3.1. Piezo-Photocatalytic Degradation in Deionized Water

The degradation of target pharmaceuticals in deionized water followed the pseudo-first-order kinetics and showed the high performance of photocatalytic (LED + Catalyst) and piezo-photocatalytic (LED + US + Catalyst) processes (Figure 3).

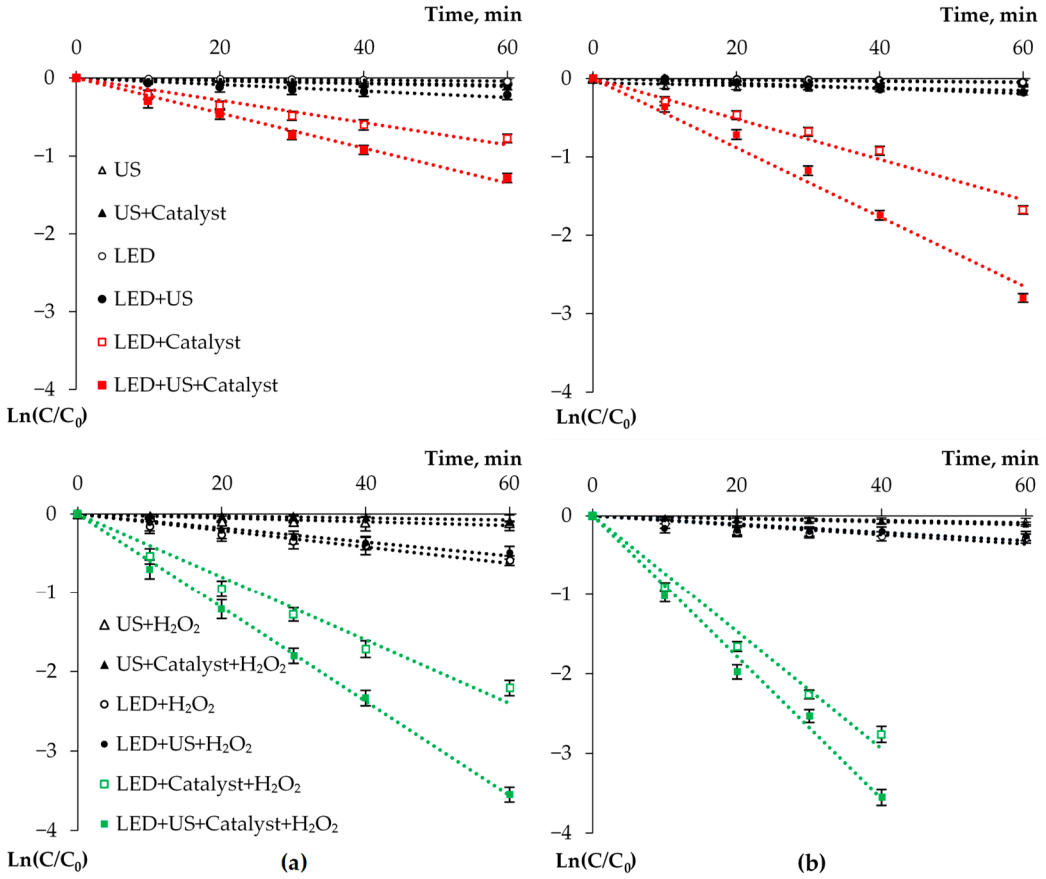

Figure 3. Degradation plots of bezafibrate (**a**) and ceftriaxone (**b**) in deionized water in the absence and presence of H_2O_2. $[Pharm]_0$ = 20 μM, $[Catalyst]_0$ = 1 g/L, $[H_2O_2]_0$ = 1 mM, pH_0 = 6.7 ± 0.2 (CFX), 5.3 ± 0.2 (BZF). Error bars represent ±SD. The enlarged control plots are shown in Supplementary Materials (Figure S1).

Control experiments revealed no degradation under irradiation with LED or ultrasound alone. Piezo-catalytic treatment (US + Catalyst) was also inefficient at a given ultrasonic intensity (0.2 W/cm^2). Simultaneous exposure to ultraviolet and ultrasonic radiation (LED + US) resulted in ~20% removal. Overall, the performance of the examined processes after 1 h exposure can be ranked as follows: LED ≈ US ≈ US + Catalyst < LED + US < LED + Catalyst < LED + US + Catalyst. Hamza et al. (2017) [30] observed only 20% decolorization of methyl orange after 1 h irradiation with visible light in the presence of calcined natural sphalerite. Raw natural sphalerite exhibited a lower photocatalytic activity and methyl orange was degraded by 82.11% in 4 h [31]. Recycling tests showed that the catalyst could be used at least three times without obvious loss of photocatalytic activity (Supplementary Materials, Figure S2). The same performance was reported earlier for the photocatalytic degradation of methylene blue using natural wolframite [32] and synthesized Cu-doped ZnS [37].

The H_2O_2-assisted piezo-photocatalytic process was also the most efficient for degrading BZF, whereas its performance for degrading CFX was similar to the photocatalytic process (Figure 3). No measurable effect of H_2O_2 was observed in the {US + H_2O_2} and {US + Catalyst + H_2O_2} systems. Adding H_2O_2 expectedly increased the degradation rate

by LED only; however, the ultrasound did not enhance the efficiency of the {LED + US + H_2O_2} process and the degradation efficiency was comparable. Table 4 presents the pseudo-first-order rate constants, which were obtained from the corresponding linear plots for photocatalytic and piezo-photocatalytic degradation with correlation coefficients above 0.95.

Table 4. The pseudo-first-order rate constants of photocatalytic and piezo-photocatalytic degradation in deionized water ($R^2 > 0.95$).

System	$k \times 10^{-2}$, min^{-1}	
	Bezafibrate	**Ceftriaxone**
LED + Catalyst	1.43 ± 0.05	2.58 ± 0.05
LED + US + Catalyst	2.25 ± 0.07	4.41 ± 0.05
LED + Catalyst + H_2O_2	4.00 ± 0.03	7.35 ± 0.02
LED + US + Catalyst + H_2O_2	5.94 ± 0.07	8.93 ± 0.06

It can be concluded that the contribution of ultrasound is significant in the absence of H_2O_2 ($k_{LED+US+catalyst} > k_{LED+catalyst}$) and decreased in the H_2O_2-assisted processes. CFX was degraded on average 1.8 times faster than BZF in all efficient catalytic systems. This indicates the higher reactivity of CFX, although the reported rate constants of •OH reaction with cephalosporin antibiotics (7.2–11 × 10^9 M^{-1} s^{-1} [42]) are comparable with the corresponding rate constant for BZF (7.4 × 10^9 M^{-1} s^{-1} [43], 8.0 × 10^9 M^{-1} s^{-1} [44]. We assume that the enhanced •OH generation in the H_2O_2-assisted systems reduced the contribution of ultrasound for CFX, which is oxidized faster than BZF under our experimental conditions. This resulted in the minor difference between *k* values between {LED + Catalyst + H_2O_2} and {LED + US + Catalyst + H_2O_2} systems (Table 4). Generally, the addition of H_2O_2 significantly increased the degradation rates and resulted in the complete removal of BZF and CFX after 1 h of treatment. Finally, the performance of control and target processes in the presence of oxidant increased in the following: US + H_2O_2 ≈ US + Catalyst + H_2O_2 < LED + H_2O_2 ≈ LED + US + H_2O_2 < LED + Catalyst + H_2O_2 < LED + US + Catalyst + H_2O_2.

Scavenging experiments also revealed the highest rate of *p*CBA decay via piezo-photocatalytic processes, and •OH exposure was quantified (Figure 4).

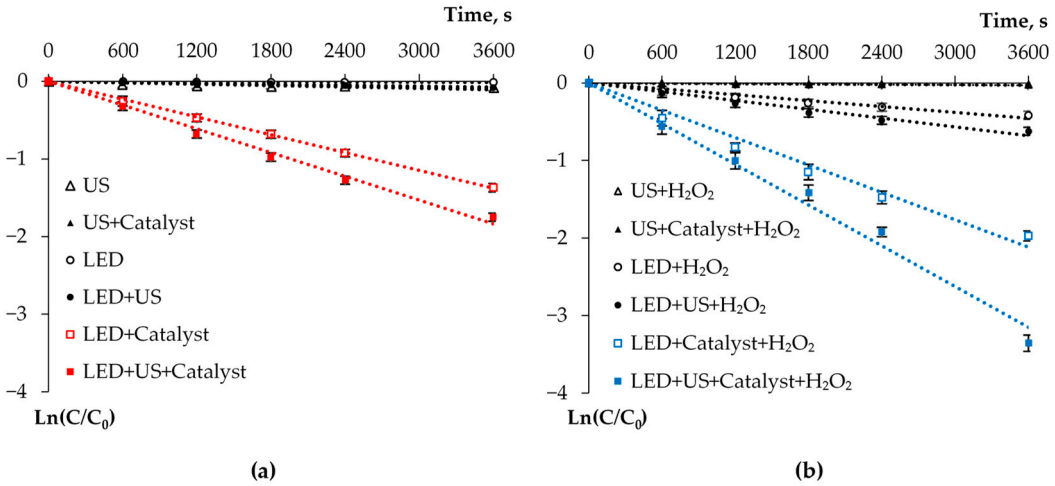

Figure 4. Decay plots of *p*CBA in deionized water in the absence (**a**) and presence (**b**) of H_2O_2. $[pCBA]_0$ = 20 μM, $[Catalyst]_0$ = 1 g/L, $[H_2O_2]_0$ = 1 mM. Error bars represent ± SD.

The estimated steady-state concentrations of •OH for piezo-photocatalytic treatment with and without H_2O_2 were 1.8 × 10^{-13} M (k_{obs} = 0.0009 s^{-1}) and 1.0 × 10^{-13} M

(k_{obs} = 0.0005 s^{-1}), respectively. The photocatalytic process (without ultrasound) showed lower decay rates and •OH exposure (Figure 4). Generally, the obtained concentrations are of the same order of magnitude as those reported earlier for the {UV + H_2O_2} system using a low-pressure mercury lamp (254 nm) ($\leq 4 \times 10^{-13}$ M, [45]; 1.0–8.0 $\times 10^{-13}$ M [46]), and also for the photocatalytic system {UV + TiO_2} with a high-pressure mercury lamp (2.74×10^{-13} M, [47]). This indicates that the piezo-photocatalytic process at 365 nm represents a competitively efficient technique relative to the conventional UV_{254} + H_2O_2 or UV_{254} + TiO_2 oxidation processes.

Figure 5 schematically depicts the proposed mechanism of H_2O_2-assisted piezo-photocatalysis under the applied conditions.

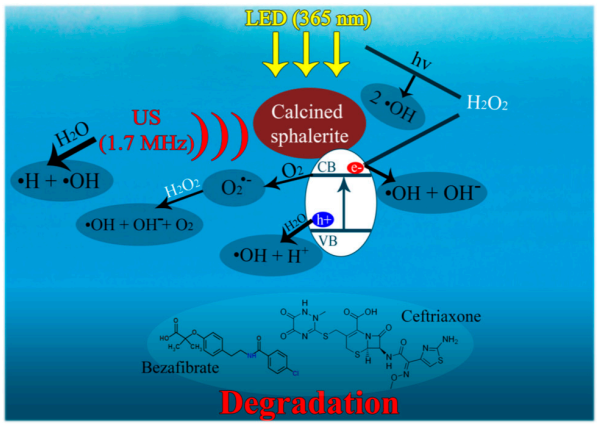

Figure 5. Schematic diagram of the piezo-photocatalytic mechanism in the presence of H_2O_2.

The additional ROS generation enhances the piezo-photocatalytic degradation in the presence of H_2O_2, which forms •OH via direct UV photolysis (1) and traps the photo-induced electrons (as electron acceptor) (2) and superoxide radical anions (3) [48–50]. H_2O_2 acts as an electron acceptor, prevents the recombination of electron–hole pairs, and accelerates their separation, thereby yielding more photo-induced holes and finally improving the photocatalytic activity [32].

3.2. Piezo-Photocatalytic Degradation in River Water

It is known that the co-existing constituents of real water matrices, such as anions and dissolved organic matter, scavenge the generated ROS, thereby inhibiting the target oxidation processes. To eliminate bicarbonates (131.2 mg/L), river water was acidified to pH 4 and 5 for the initial experiments without added oxidant. The results showed that pre-acidification barely improved the photocatalytic (LED + Catalyst) and piezo-photocatalytic (LED + US + Catalyst) degradation of BZF (Figure 6).

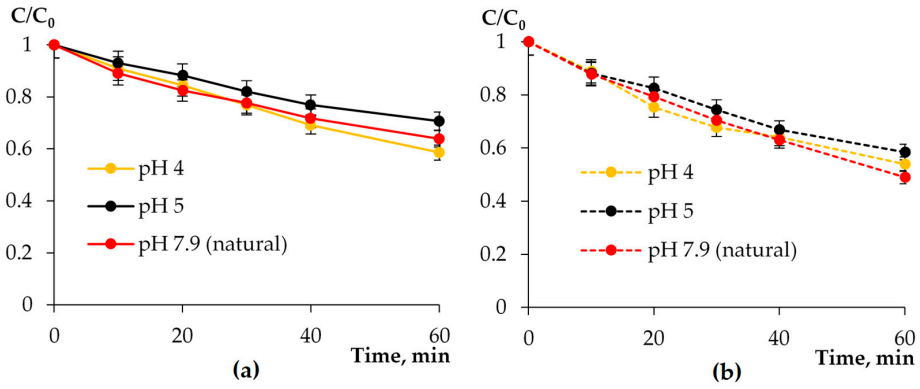

Figure 6. Effect of pH on the degradation of bezafibrate in river water by photo- (**a**) and piezo-photocatalytic (**b**) processes. $[BZF]_0$ = 20 µM. Error bars represent ±SD.

The obtained kinetics revealed roughly the same pseudo-first-order constants as those obtained at natural pH 7.9 (0.8 and 1.2 min^{-1}). Therefore, further experiments, including control series (LED, US, US + Catalyst, LED + US), were performed at unadjusted pH, which is technologically more favorable to avoid a pre-acidification step. Similar to deionized water, the high performance of photo- and piezo-photocatalytic processes was observed in river water (Figure 7).

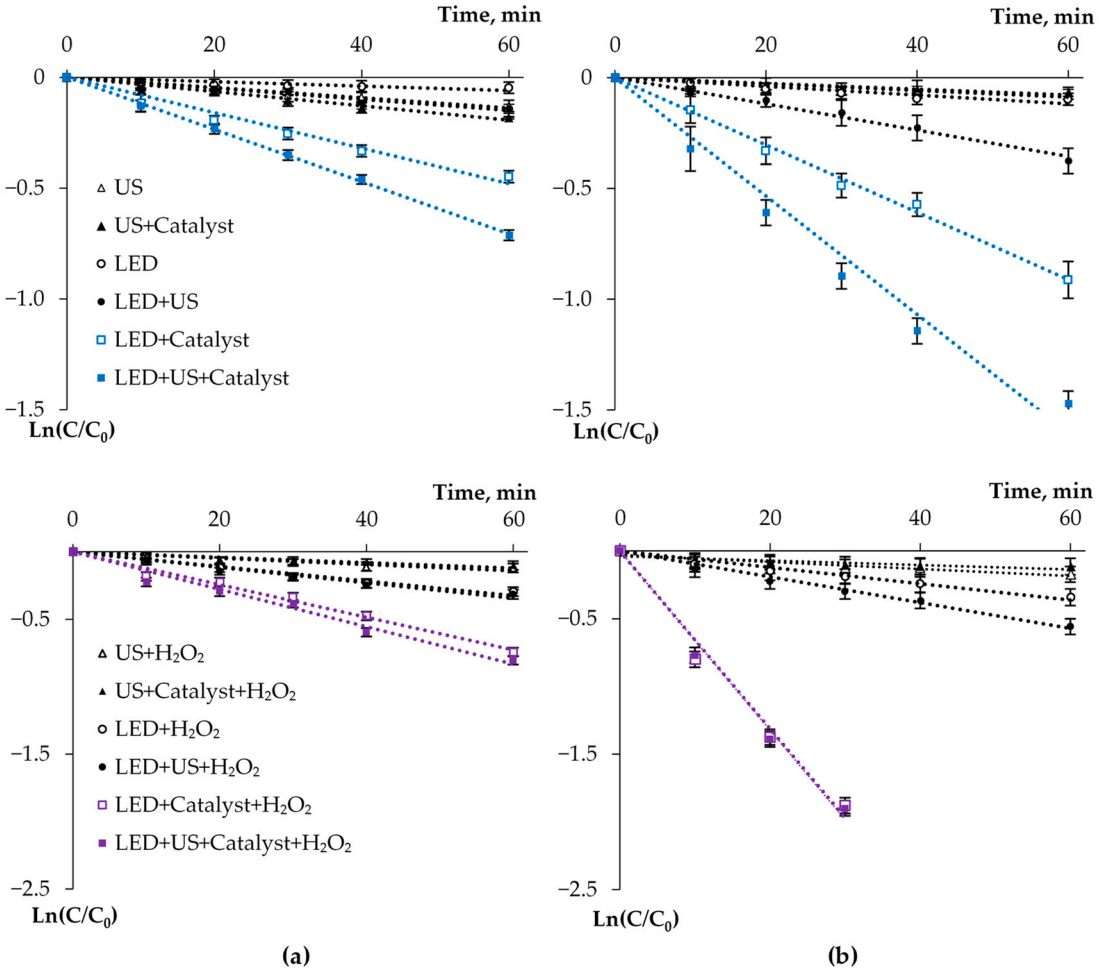

Figure 7. Degradation plots of bezafibrate (**a**) and ceftriaxone (**b**) in river water in the absence and presence of H_2O_2. $[Pharm]_0$ = 20 μM, $[Catalyst]_0$ = 1 g/L, $[H_2O_2]_0$ = 1 mM, pH_0 = 8.0 ± 0.1. Error bars represent ±SD. The enlarged control plots are shown in Supplementary Materials (Figure S3).

Control experiments under catalyst-free conditions and piezo-catalytic exposure (US + Catalyst) showed significantly lower efficiency. Meanwhile, the degradation rates of BZF and CFX in river water without added H_2O_2 decreased by 1.7 times as compared to those observed in deionized water. Such an inhibition effect was observed for both photo- and piezo-photocatalytic processes (Table 5).

This is due to the interfering influence of co-existing constituents, primarily bicarbonates and sulfates, which scavenge •OH with constants of 8.5×10^6 M^{-1} s^{-1} [51] (3) and 1.5×10^8 M^{-1} s^{-1} [52] (4):

$$OH\bullet + HCO_3^- \rightarrow CO_3\bullet^- + H_2O \quad (3)$$

$$OH\bullet + SO_4^{2-} \rightarrow SO_4\bullet^- + OH^- \quad (4)$$

Table 5. The pseudo-first-order rate constants of photocatalytic and piezo-photocatalytic degradation in river water ($R^2 > 0.95$).

System	$k \times 10^{-2}$, min^{-1}	
	Bezafibrate	**Ceftriaxone**
LED + Catalyst	0.80 ± 0.05	1.52 ± 0.04
LED + US + Catalyst	1.18 ± 0.05	2.67 ± 0.05
LED + Catalyst + H_2O_2	1.21 ± 0.06	6.56 ± 0.06
LED + US + Catalyst + H_2O_2	1.39 ± 0.05	6.61 ± 0.06

The scavenging effect of dissolved organic matter ($k_{DOC, OH\bullet} = 2.5 \times 10^4$ mgC^{-1} s^{-1} L [53]) appears to be rather weak due to its relatively low level (2.1 mgDOC/L). Despite the inhibition, the piezo-photocatalytic process kept the best performance for both compounds, attaining 77% and 48% removal of CFX and BZF after 1 h exposure, respectively. Similar to deionized water, the obtained degradation rate constants for piezo-photocatalysis (LED + US + Catalyst) were 1.6–1.7 times higher than those observed for photo-catalysis (LED + Catalyst) (Table 5).

Adding H_2O_2 hid the contribution of ultrasound to the degradation of pharmaceuticals with similar rate constants in the {LED + Catalyst + H_2O_2} and {LED + US + Catalyst + H_2O_2} systems (Table 5). However, the oxidant improved the removal efficiency to 100% and 55% for CFX and BZF after 1 h exposure, respectively. Similar to deionized water, BZF was more resistant to degradation in river water. The mean residual concentration of H_2O_2 was 0.46 ± 0.03 mM (54% consumption), slightly lower than in deionized water (Supplementary Materials, Figure S4). This level is higher than the EC_{50}/LD_{50} values for aquatic biota, such as the algae *Skeletonema costatum* (0.041 mM) and the crustacean *Brachionus plicatilis* (0.071 mM), but comparable with those for freshwater fish *Pimephales promelas* (0.482 mM) [54]. Meanwhile, high doses of H_2O_2 (up to 2.5 mL of 30% H_2O_2 per liter) might be applied for wastewater treatment and improve biodegradability [55]. As such, if the H_2O_2-assisted piezo-photocatalytic method is used as a pretreatment step, the subsequent biotreatment could completely degrade the residual H_2O_2 at ppm level. The residual H_2O_2 cannot be recycled under the experimental conditions applied but can be further decomposed over our catalyst or other ZnO-based catalysts [56], as well as catalase [57], goethite, or ferric hydroxide [58].

The rates of *p*CBA decay in river water were about one order of magnitude lower than those obtained in deionized water (Figure 8).

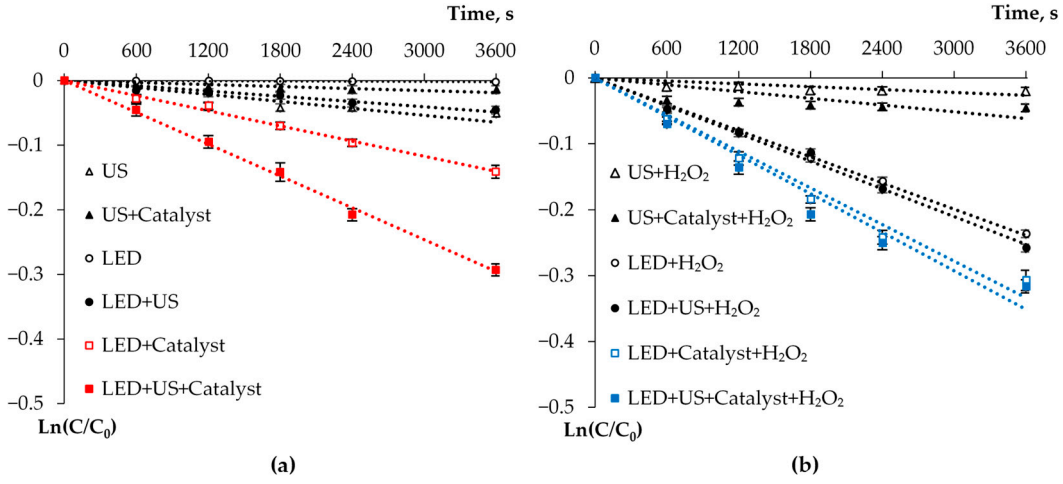

Figure 8. Decay plots of *p*CBA in river water in the absence (**a**) and presence (**b**) of H_2O_2. $[pCBA]_0$ = 20 µM, $[Catalyst]_0$ = 1 g/L, $[H_2O_2]_0$ = 1 mM. Error bars represent ±SD.

Accordingly, the $[\bullet OH]_{ss}$ values for the piezo-photocatalytic process were on the order of 10^{-14} M. However, similar to BZF and CFX degradation, piezo-photocatalysis was more effective than photocatalysis; adding H_2O_2 also hid the contribution of ultrasound, and the performance of piezo-photocatalysis and photocatalysis was comparable.

3.3. Synergistic Effect

Piezo-photocatalysis may exhibit a synergistic effect that provides better performance than the sum of processes performed individually. A synergy between piezocatalytic and photocatalytic processes can be estimated through the synergistic factor (SF) or index in terms of removal efficiency (RE) [59] (5):

$$SF = \frac{\%\ RE_{LED+US+catalyst}}{\%\ RE_{LED+catalyst} + \%\ RE_{US+catalyst}} \quad (5)$$

The obtained SF values for degrading target pharmaceuticals in the absence and presence of H_2O_2 were 1.0–1.2, indicating the additive (=1) and mild synergistic (slightly >1) effects. Based on this approach, other studies on the piezo-photocatalytic degradation of pharmaceuticals also reported relatively low SF values of 0.7–1.7 [59], 1–1.5 [18], and 1.0449 [15]. Phenol was also degraded via the UV + US + ZnO process with low factors of 1.24–1.25 [60,61]. An additive effect was found for the degradation of diclofenac [62] and norflurazon [63] using Fe-ZnO and Au-ZnO, respectively. However, a synergistic effect without giving SF values was recently reported for mineralizing diclofenac [14] and degrading tetracycline [10].

Another body of literature mainly deals with organic dyes and supports the existence of synergy in the ZnO-based piezo-photocatalysis using different approaches [64–75]. We propose that applying the high-intensity ultrasound at 1.7 MHz for large-scale applications could enhance the synergistic effect.

Adding H_2O_2 increased the degradation rates while keeping an additive effect for degrading BZF in deionized water (SF = 1). Synergy can be hardly evaluated in other H_2O_2-assisted piezo-photocatalytic systems (for removing BZF from natural water and CFX from both water matrices) due to the hidden contribution of ultrasound ($k_{LED+Catalyst+}H_2O_2 \approx k_{LED+US+Catalyst+}H_2O_2$). No synergy was evident in the {UV + US + ZnO + H_2O_2} system for degrading salicylic acid [18] and Reactive Yellow dye [76]. Another dye (acid orange 7) was also degraded via H_2O_2-mediated piezo-photocatalysis with a low SF of 1.10 [77]. Other literature reports the synergy of the US + UV + ZnO + H_2O_2 process for degrading malachite green dye [78] and antibiotic ofloxacin with an SF of 3.10 [79]. It should be emphasized that the fabricated ZnO and its various (nano)composites along with low-frequency ultrasound (20–45 kHz) were utilized in the aforementioned research.

Despite the absence of a high synergistic effect (as also observed in many previous studies), H_2O_2-assisted processes exhibited the best performance for the rapid degradation of target pharmaceuticals in deionized water. Moreover, this hybrid process was also efficient for degrading pharmaceuticals in river water, and its performance could be synergistically boosted by increasing the ultrasonic intensity and generating more ROS. Since ultrasound is much less absorbed by turbid water as compared to ultraviolet radiation, piezo-photocatalysis is supposed to be more beneficial than photocatalysis for treating real water.

4. Conclusions

This study demonstrates that the calcined natural sphalerite (mainly ZnO) represents a good alternative to the fabricated ZnO-based catalysts and can be successfully employed in piezo-photocatalytic processes for water treatment. Piezo-photocatalysis based on high-frequency ultrasound (1.7 MHz) and UV LED (365 nm) was the most efficient process for degrading the pharmaceuticals bezafibrate and ceftriaxone in both ultrapure (deionized) and real (river) water at unadjusted pH. Adding H_2O_2 improved the performance of piezo-photocatalysis, but the contribution of ultrasound at a given intensity was negligible in

river water. Ceftriaxone was degraded significantly faster than bezafibrate in all examined systems. Although only a mild synergy between piezo- and photocatalytic processes was observed in this study, H_2O_2-assisted piezo-photocatalysis using calcined natural sphalerite can be considered an efficient green method for degrading pharmaceuticals in real waters. We anticipate the scaling up and further development of this cost-effective method using UVA LEDs, high-frequency ultrasound, and natural photoactive piezoelectric minerals.

Supplementary Materials: The following supporting information can be downloaded at: https://www.mdpi.com/article/10.3390/w15173092/s1, Figure S1: Control plots of bezafibrate (a) and ceftriaxone (b) degradation in deionized water in the absence and presence of H_2O_2. $[Pharm]_0$ = 20 μM, $[Catalyst]_0$ = 1 g/L, $[H_2O_2]_0$ = 1 mM, pH_0 = 6.7 ± 0.2 (CFX), 5.3 ± 0.2 (BZF). Error bars represent ±SD; Figure S2: Recycling tests for the photocatalytic (LED + Catalyst) degradation of bezafibrate in deionized water using calcined sphalerite. $[BZF]_0$ = 20 μM, $[Catalyst]_0$ = 1 g/L; Figure S3: Control plots of bezafibrate (a) and ceftriaxone (b) degradation in river water in the absence and presence of H_2O_2. $[Pharm]_0$ = 20 μM, $[Catalyst]_0$ = 1 g/L, $[H_2O_2]_0$ = 1 mM, pH_0 = 8.0 ± 0.1. Error bars represent ±SD; Figure S4: Consumption of H_2O_2 after 1 h photocatalytic exposure. $[Pharm]_0$ = 20 μM, $[Catalyst]_0$ = 1 g/L, $[H_2O_2]_0$ = 1 mM.

Author Contributions: Investigation, formal analysis, and validation, S.P., V.T. and E.P.; project administration, methodology, data curation, and writing—original draft preparation, G.M.; conceptualization, methodology, supervision, and writing—review and editing, V.B. All authors have read and agreed to the published version of the manuscript.

Funding: This research was funded by the Russian Science Foundation, grant number 22-23-00425.

Data Availability Statement: Data is contained within the article and Supplementary Materials.

Conflicts of Interest: The authors declare no conflict of interest.

References

1. World Health Organization. Drinking Water, Key Facts. Available online: https://www.who.int/news-room/fact-sheets/detail/drinking-water (accessed on 27 June 2023).
2. Wilkinson, J.L.; Boxall, A.B.A.; Kolpin, D.W.; Leung, K.M.Y.; Lai, R.W.S.; Galbán-Malagón, C.; Adell, A.D.; Mondon, J.; Metian, M.; Marchant, R.A.; et al. Pharmaceutical pollution of the world's rivers. *Proc. Natl. Acad. Sci. USA* **2022**, *119*, e2113947119. [CrossRef]
3. Jiang, Z.; Tan, X.; Huang, Y. Piezoelectric effect enhanced photocatalysis in environmental remediation: State-of-the-art techniques and future scenarios. *Sci. Total Environ.* **2022**, *806*, 150924. [CrossRef] [PubMed]
4. Li, J.; Liu, X.; Zhao, G.; Liu, Z.; Cai, Y.; Wang, S.; Shen, C.; Hu, B.; Wang, X. Piezoelectric materials and techniques for environmental pollution remediation. *Sci. Total Environ.* **2023**, *869*, 161767. [CrossRef] [PubMed]
5. Liu, J.; Qi, W.; Xu, M.; Thomas, T.; Liu, S.; Yang, M. Piezocatalytic techniques in environmental remediation. *Angew. Chem. Int. Ed.* **2023**, *62*, e202213927. [CrossRef] [PubMed]
6. Nie, G.; Yao, Y.; Duan, X.; Xiao, L.; Wang, S. Advances of piezoelectric nanomaterials for applications in advanced oxidation technologies. *Curr. Opin.* **2021**, *33*, 100693. [CrossRef]
7. Wang, Z.L.; Song, J. Piezoelectric nanogenerators based on zinc oxide nanowire arrays. *Science* **2006**, *312*, 242–245. [CrossRef]
8. Asli, S.A.; Taghizadeh, M. Sonophotocatalytic degradation of pollutants by ZnO-based catalysts: A review. *ChemistrySelect* **2020**, *5*, 13720–13731. [CrossRef]
9. Dhull, P.; Sudhaik, A.; Raizada, P.; Thakur, S.; Nguyen, V.-H.; Van Le, Q.; Kumar, N.; Khan, A.A.P.; Marwani, H.M.; Selvasembian, R.; et al. An overview on ZnO-based sonophotocatalytic mitigation of aqueous phase pollutants. *Chemosphere* **2023**, *333*, 138873. [CrossRef]
10. Gao, Q.; Zhou, L.; Xu, S.; Dai, S.; Zhu, Q.; Li, Y. Significant improvement and mechanism of tetracycline degradation with the synergistic piezoelectric effect of ZnO/CuS Z-scheme heterojunction photocatalysts. *Environ. Sci. Nano* **2023**, *10*, 581–594. [CrossRef]
11. Bembibre, A.; Benamara, M.; Hjiri, M.; Gómez, E.; Alamri, H.R.; Dhahri, R.; Serrá, A. Visible-light driven sonophotocatalytic removal of tetracycline using Ca-doped ZnO nanoparticles. *Chem. Eng. J.* **2022**, *427*, 132006. [CrossRef]
12. Khitab, F.; Shah, J.; Rasul, J.M. Systematic assessment of visible light driven photocatalysts for the removal of cefixime in aqueous solution sonophotocatalytically. *Int. J. Environ. Anal. Chem.* **2022**, 1–20. [CrossRef]
13. Liu, J.; Chen, J.; Wu, Z.; Zhu, K.; Wang, J.; Li, Z.; Tai, G.; Liu, X.; Lu, S. Enhanced visible-light photocatalytic performances of ZnO through loading AgI and coupling piezo-photocatalysis. *J. Alloys Compd.* **2021**, *852*, 156848. [CrossRef]
14. Meroni, D.; Bianchi, C.L.; Boffito, D.C.; Cerrato, G.; Bruni, A.; Sartirana, M.; Falletta, E. Piezo-enhanced photocatalytic diclofenac mineralization over ZnO. *Ultrason. Sonochem.* **2021**, *75*, 105615. [CrossRef] [PubMed]

15. Moradi, S.; Sobhgol, S.A.; Hayati, F.; Isari, A.A.; Kakavandi, B.; Bashardoust, P.; Anvaripour, B. Performance and reaction mechanism of MgO/ZnO/Graphene ternary nanocomposite in coupling with LED and ultrasound waves for the degradation of sulfamethoxazole and pharmaceutical wastewater. *Sep. Purif. Technol.* **2020**, *251*, 117373. [CrossRef]
16. Almasi, A.; Mohammadi, M.; Baniamerian, F.; Berizi, Z.; Almasi, M.H.; Pariz, Z. Modeling of antibiotic degradation in sonophotocatalytic process, increasing biodegradability and process optimization by response surface methodology (RSM). *Int. J. Environ. Sci. Technol.* **2019**, *16*, 8437–8448. [CrossRef]
17. Almasi, A.; Mohammadi, M.; Shamsi, K.; Mohammadi, S.; Saeidimoghadam, Z. Sonolytic and photocatalytic (sonophotocatalytic) removal of cephalexin from aqueous solution: Process optimization using response surface methodology (RSM). *Desalination Water Treat.* **2017**, *85*, 256–263. [CrossRef]
18. Fatimah, I.; Pradita, R.Y.; Nurfalinda, A. Study on ZnO catalytic activity in salycilic acid degradation by sonophotocatalysis. *Chem. Eng. Trans.* **2017**, *56*, 1651–1656. [CrossRef]
19. Mason, T.J.; Cobley, A.J.; Graves, J.E.; Morgan, D. New evidence for the inverse dependence of mechanical and chemical effects on the frequency of ultrasound. *Ultrason. Sonochem.* **2011**, *18*, 226–230. [CrossRef]
20. Matafonova, G.; Batoev, V. Review on low- and high-frequency sonolytic, sonophotolytic and sonophotochemical processes for inactivating pathogenic microorganisms in aqueous media. *Water Res.* **2019**, *166*, 115085. [CrossRef]
21. Garkusheva, N.; Tsenter, I.; Kobunova, E.; Matafonova, G.; Batoev, V. Dual-frequency ultrasonic inactivation of *Escherichia coli* and *Enterococcus faecalis* using persulfate: A synergistic effect. *Water* **2022**, *14*, 2604. [CrossRef]
22. Laurenti, M.; Garino, N.; Canavese, G.; Simelys, H.; Valentina, C. Piezo- and photocatalytic activity of ferroelectric ZnO:Sb thin films for the efficient degradation of Rhodamine-ß dye pollutant. *Appl. Mater. Interfaces* **2020**, *12*, 25798–25808. [CrossRef] [PubMed]
23. Chen, Y.; Lu, A.; Li, Y.; Zhang, L.; Yip, H.Y.; Zhao, H.; An, T.; Wong, P.-K. Naturally occurring sphalerite as a novel cost-effective photocatalyst for bacterial disinfection under visible light. *Environ. Sci. Technol.* **2011**, *45*, 5689–5695. [CrossRef] [PubMed]
24. Li, Y.; Ding, C.; Liu, Y.; Li, Y.; Lu, A.; Wang, C.; Ding, H. Visible light photocatalysis of natural semiconducting minerals, Chapter 2. In *Advances in Photocatalytic Disinfection, Green Chemistry and Sustainable Technology*; An, T., Zhao, H., Wong, P.K., Eds.; Springer: Berlin/Heidelberg, Germany, 2017; pp. 17–39. [CrossRef]
25. Moradi, M.; Kalantary, R.R.; Esrafili, A.; Jafari, A.J.; Gholami, M. Visible light photocatalytic inactivation of *Escherichia coli* by natural pyrite assisted by oxalate at neutral pH. *J. Mol. Liq.* **2017**, *248*, 880–889. [CrossRef]
26. Peng, X.; Ng, T.W.; Huang, G.; Wang, W.; An, T.; Wong, P.K. Bacterial disinfection in a sunlight/visible-light-driven photocatalytic reactor by recyclable natural magnetic sphalerite. *Chemosphere* **2017**, *166*, 521–527. [CrossRef]
27. Xia, D.; Ng, T.W.; An, T.; Li, G.; Li, Y.; Yip, H.Y.; Zhao, H.; Lu, A.; Wong, P.-K. A recyclable mineral catalyst for visible-light-driven photocatalytic inactivation of bacteria: Natural magnetic sphalerite. *Environ. Sci. Technol.* **2013**, *47*, 11166–11173. [CrossRef] [PubMed]
28. Xia, D.; Liu, H.; Jiang, Z.; Ng, T.W.; Lai, W.S.; An, T.; Wang, W.; Wong, P.K. Visible-light-driven photocatalytic inactivation of *Escherichia coli* K-12 over thermal treated natural magnetic sphalerite: Band structure analysis and toxicity evaluation. *Appl. Catal. B* **2018**, *224*, 541–552. [CrossRef]
29. García-Muñoz, P.; López-Maxías, C.; Guerra-Rodríguez, S.; Carbajo, J.; Casas, J.A.; Rodríguez-Chueca, J. Photocatalytic activation of peroxymonosulfate using ilmenite ($FeTiO_3$) for *Enterococcus faecalis* inactivation. *J. Environ. Chem. Eng.* **2022**, *10*, 108231. [CrossRef]
30. Hamza, A.; John, I.J.; Mukhtar, B. Enhanced photocatalytic activity of calcined natural sphalerite under visible light irradiation. *J. Mater. Res. Technol.* **2017**, *6*, 1–6. [CrossRef]
31. Shen, C.; Gu, X.; Yang, B.; Zhang, D.; Wang, Z.; Shu, Z.; Dick, J.; Lu, A. Mineralogical characteristics and photocatalytic properties of natural sphalerite from China. *J. Environ. Sci.* **2020**, *89*, 156–166. [CrossRef]
32. Li, L.; Li, Y.; Li, Y.; Lu, A.; Ding, H.; Wong, P.K.; Sun, H.; Shi, J. Natural wolframite as a novel visible-light photocatalyst towards organics degradation and bacterial inactivation. *Catal. Today* **2020**, *358*, 177–183. [CrossRef]
33. Moradi, M.; Naderi, A.; Bahari, N.; Harati, M.; Rodríguez-Chueca, J.; Kalantary, R.R. Visible-light-driven photocatalytic inactivation of *Escherichia coli* by titanium dioxide anchored on natural pyrite. *Inorg. Chem. Commun.* **2022**, *144*, 109913. [CrossRef]
34. Ayed, S.B.; Mansour, L.; Vaiano, V.; Harrath, A.H.; Ayari, F.; Rizzo, L. Magnetic Fe_3O_4-natural iron ore/calcium alginate beads as heterogeneous catalyst for Novacron blue dye degradation in water by (photo) Fenton process. *J. Photochem. Photobiol. A* **2023**, *438*, 114566. [CrossRef]
35. Peighambardoust, S.J.; Boffito, D.C.; Foroutan, R.; Ramavandi, B. Sono-photocatalytic activity of sea sediment@400/ZnO catalyst to remove cationic dyes from wastewater. *J. Mol. Liq.* **2022**, *367*, 120478. [CrossRef]
36. Popova, S.; Tazetdinova, V.; Pavlova, E.; Matafonova, G.; Batoev, V. Characteristics and sonophotocatalytic activity of natural sphalerite under ultrasonic (1.7 MHz) and UVA LED (365 nm) irradiation. *Materials* **2022**, *15*, 5412. [CrossRef]
37. Xiong, G.; Wang, Y.; Sun, Y.; You, L.; Ren, B.; Xu, Z.; He, Y.; Ruhlmann, L.; Ding, F. Sphalerite Cu/ZnS nanoparticles derived from Cu/Zn-ZIF-8 for the photocatalytic degradation and adsorption of dyes. *Eur. J. Inorg. Chem.* **2018**, *2018*, 1038–1046. [CrossRef]
38. Fatimah, I.; Purwiandono, G.; Sahroni, I.; Sagadevan, S.; Chun-Oh, W.; Ghazali, S.A.I.S.M.; Doong, R. Recyclable catalyst of ZnO/SiO_2 prepared from Salacca leaves ash for sustainable biodiesel conversion. *S. Afr. J. Chem. Eng.* **2022**, *40*, 134–143. [CrossRef]

39. Elovitz, M.S.; von Gunten, U. Hydroxyl radical/ozone ratios during ozonation processes. I. The R_{ct} concept. *Ozone Sci. Eng.* **1999**, *21*, 239–260. [CrossRef]
40. Lipps, W.C.; Baxter, T.E.; Braun-Howland, E. (Eds.) *Standard Methods For the Examination of Water and Wastewater*; APHA Press: Washington, DC, USA, 2017.
41. Eisenberg, G. Colorimetric determination of hydrogen peroxide. *Ind. Eng. Chem. Anal. Ed.* **1943**, *15*, 327–328. [CrossRef]
42. Wojnárovits, L.; Tóth, T.; Takács, E. Critical evaluation of rate coefficients for hydroxyl radical reactions with antibiotics: A review. *Crit. Rev. Environ. Sci. Technol.* **2018**, *48*, 575–613. [CrossRef]
43. Huber, M.M.; Canonica, S.; Park, G.-Y.; von Gunten, U. Oxidation of pharmaceuticals during ozonation and advanced oxidation processes. *Environ. Sci. Technol.* **2003**, *37*, 1016–1024. [CrossRef] [PubMed]
44. Razavi, B.; Song, W.; Cooper, W.J.; Greaves, J.; Jeong, J. Free-radical-induced oxidative and reductive degradation of fibrate pharmaceuticals: Kinetic studies and degradation mechanisms. *J. Phys. Chem. A* **2009**, *113*, 1287–1294. [CrossRef] [PubMed]
45. Luo, C.; Ma, J.; Jiang, J.; Liu, Y.; Song, Y.; Yang, Y.; Guan, Y.; Wu, D. Simulation and comparative study on the oxidation kinetics of atrazine by UV/H_2O_2, UV/HSO_5^- and UV/$S_2O_8^{2-}$. *Water Res.* **2015**, *80*, 99–108. [CrossRef] [PubMed]
46. Ulliman, S.L.; McKay, G.; Rosario-Ortiz, F.L.; Linden, K.G. Low levels of iron enhance UV/H_2O_2 efficiency at neutral pH. *Water Res.* **2018**, *130*, 234–242. [CrossRef] [PubMed]
47. Tang, T.; Lu, G.; Wang, W.; Wang, R.; Huang, K.; Qiu, Z.; Tao, X.; Dang, Z. Photocatalytic removal of organic phosphate esters by TiO_2: Effect of inorganic ions and humic acid. *Chemosphere* **2018**, *206*, 26–32. [CrossRef]
48. Armaković, S.J.; Armaković, S.; Finčur, N.L.; Šibul, F.; Vione, D.; Šetrajčić, J.P.; Abramović, B.F. Influence of electron acceptors on the kinetics of metoprolol photocatalytic degradation in TiO_2 suspension. A combined experimental and theoretical study. *RSC Adv.* **2015**, *5*, 54589–54604. [CrossRef]
49. Monteagudo, J.M.; Durán, A.; San Martín, I.; Vellón, B. Photocatalytic degradation of aniline by solar/TiO_2 system in the presence of the electron acceptors $Na_2S_2O_8$ and H_2O_2. *Sep. Purif. Technol.* **2020**, *238*, 116456. [CrossRef]
50. Rahmati, R.; Nayebi, B.; Ayati, B. Investigating the effect of hydrogen peroxide as an electron acceptor in increasing the capability of slurry photocatalytic process in dye removal. *Water Sci. Technol.* **2021**, *83*, 2414–2423. [CrossRef]
51. Buxton, G.V.; Elliot, A.J. Rate constant for reaction of hydroxyl radicals with bicarbonate ions. *Int. J. Radiat. Appl. Instrum. C* **1986**, *27*, 241–243. [CrossRef]
52. Grčić, I.; Vujević, D.; Koprivanac, N. Modeling the mineralization and discoloration in colored systems by (US)Fe^{2+}/H_2O_2/$S_2O_8^{2-}$ processes: A proposed degradation pathway. *Chem. Eng. J.* **2010**, *157*, 35–44. [CrossRef]
53. Larson, R.A.; Zepp, R.G. Reactivity of the carbonate radical with aniline derivatives. *Environ. Toxicol. Chem.* **1988**, *7*, 265–274. [CrossRef]
54. Sunday, M.O.; Jadoon, W.A.; Ayeni, T.T.; Iwamoto, Y.; Takeda, K.; Imaizumi, Y.; Arakaki, T.; Sakugawa, H. Heterogeneity and potential aquatic toxicity of hydrogen peroxide concentrations in selected rivers across Japan. *Sci. Total Environ.* **2020**, *733*, 139349. [CrossRef] [PubMed]
55. Ksibi, M. Chemical oxidation with hydrogen peroxide for domestic wastewater treatment. *Chem. Eng. J.* **2006**, *119*, 161–165. [CrossRef]
56. Salem, I. Catalytic decomposition of H_2O_2 over supported ZnO. *Monatshefte Für Chem.* **2000**, *131*, 1139–1150. [CrossRef]
57. Yoon, D.S.; Won, K.; Kim, Y.H.; Song, B.K.; Kim, S.J.; Moon, S.J.; Kim, B.S. Continuous removal of hydrogen peroxide with immobilised catalase for wastewater reuse. *Water Sci. Technol.* **2007**, *55*, 27–33. [CrossRef]
58. A Process for Removal of Hydrogen Peroxide from an Aqueous Solution. Patent WO2014012949A1, 23 January 2014. Available online: https://patentimages.storage.googleapis.com/4f/6c/f9/b24eb7f85a1d00/WO2014012949A1.pdf (accessed on 22 August 2023).
59. Liu, P.; Wu, Z.; Abramova, A.V.; Cravotto, G. Sonochemical processes for the degradation of antibiotics in aqueous solutions: A review. *Ultrason. Sonochem.* **2021**, *74*, 105566. [CrossRef]
60. Anju, S.G.; Yesodharan, S.; Yesodharan, E.P. Zinc oxide mediated sonophotocatalytic degradation of phenol in water. *Chem. Eng. J.* **2012**, *189–190*, 84–93. [CrossRef]
61. Fatimah, I.; Novitasari. Preparation of TiO_2-ZnO and its activity test in sonophotocatalytic degradation of phenol. *IOP Conf. Ser. Mater. Sci. Eng.* **2016**, *107*, 012003. [CrossRef]
62. Madhavan, J.; Sathish Kumar, P.S.; Anandan, S.; Zhou, M.; Grieser, F.; Ashokkumar, M. Ultrasound assisted photocatalytic degradation of diclofenac in an aqueous environment. *Chemosphere* **2010**, *80*, 747–752. [CrossRef]
63. Sathishkumar, P.; Mangalaraja, R.V.; Rozas, O.; Vergara, C.; Mansilla, H.D.; Gracia-Pinilla, M.A.; Anandan, S. Sonophotocatalytic mineralization of Norflurazon in aqueous environment. *Chemosphere* **2016**, *146*, 216–225. [CrossRef]
64. Talebian, N.; Nilforoushan, M.R.; Mogaddas, F.J. Comparative study on the sonophotocatalytic degradation of hazardous waste. *Ceram. Int.* **2013**, *39*, 4913–4921. [CrossRef]
65. Kumar, R.; Kumar, G.; Akhtar, M.S.; Umar, A. Sonophotocatalytic degradation of methyl orange using ZnO nano-aggregates. *J. Alloys Compd.* **2015**, *629*, 167–172. [CrossRef]
66. Ertugay, N.; Acar, F.N. Ultrasound and UV stimulated heterogeneous catalytic oxidation of an azo dye: A synergistic effect. *Prog. React. Kinet. Mech.* **2017**, *42*, 235–243. [CrossRef]

67. Lops, C.; Ancona, A.; Di Cesare, K.; Dumontel, B.; Garino, N.; Canavese, G.; Hérnandez, S.; Cauda, V. Sonophotocatalytic degradation mechanisms of Rhodamine B dye via radicals generation by micro- and nano-particles of ZnO. *Appl. Catal. B* **2019**, *243*, 629–640. [CrossRef] [PubMed]
68. Ma, J.; Ren, J.; Jia, Y.; Wu, Z.; Chen, L.; Haugen, N.O.; Huang, H.; Liu, Y. High efficiency bi-harvesting light/vibration energy using piezoelectric zinc oxide nanorods for dye decomposition. *Nano Energy* **2019**, *62*, 376–383. [CrossRef]
69. Asgari, G.; Shabanloo, A.; Salari, M.; Eslami, F. Sonophotocatalytic treatment of AB113 dye and real textile wastewater using ZnO/persulfate: Modeling by response surface methodology and artificial neural network. *Environ. Res.* **2020**, *184*, 109367. [CrossRef]
70. Khairy, M.; Naguib, E.M.; Mohamed, M.M. Enhancement of photocatalytic and sonophotocatalytic degradation of 4-nitrophenol by ZnO/graphene oxide and ZnO/carbon nanotube nanocomposites. *J. Photochem. Photobiol. A* **2020**, *396*, 112507. [CrossRef]
71. Xiang, D.; Liu, Z.; Wu, M.; Liu, H.; Zhang, X.; Wang, Z.; Wang, Z.L.; Li, L. Enhanced piezo-photoelectric catalysis with oriented carrier migration in asymmetric Au-ZnO nanorod array. *Small* **2020**, *16*, 1907603. [CrossRef]
72. Li, Y.; Chen, H.; Wang, L.; Wu, T.; Wu, Y.; He, Y. $KNbO_3$/ZnO heterojunction harvesting ultrasonic mechanical energy and solar energy to efficiently degrade methyl orange. *Ultrason. Sonochem.* **2021**, *78*, 105754. [CrossRef]
73. Yang, R.; Wu, Z.; Yang, Y.; Li, Y.; Zhang, L.; Yu, B. Understanding the origin of synergistic catalytic activities for ZnO based sonophotocatalytic degradation of methyl orange. *J. Taiwan Inst. Chem. Eng.* **2021**, *119*, 128–135. [CrossRef]
74. Zarazúa-Morín, M.E.; Galindo-Luna, A.S.; Gallegos-Sánchez, V.J.; Zermeño-Resendiz, B.B.; Torres-Martínez, L.M. Novel hydrothermal-assisted microwave synthesis of $NiTiO_3$/ZnO and sonophotocatalytic effect for degradation of rhodamine B. *Top. Catal.* **2022**, *65*, 1182–1190. [CrossRef]
75. Naderi, A.; Firooz, M.H.; Gharibzadeh, F.; Giannakis, S.; Ahmadi, M.; Kalantary, R.R.; Kakavandi, B. Anchoring ZnO on spinel cobalt ferrite for highly synergic sono-photo-catalytic, surfactant-assisted PAH degradation from soil washing solutions. *J. Environ. Manag.* **2023**, *326*, 116584. [CrossRef] [PubMed]
76. Eren, Z. Degradation of an azo dye with homogeneous and heterogeneous catalysts by sonophotolysis. *Clean Soil Air Water* **2012**, *40*, 1284–1289. [CrossRef]
77. Wei, H.; Rahaman, M.H.; Zhao, J.; Lia, D.; Zhai, J. Hydrogen peroxide enhanced sonophotocatalytic degradation of acid orange 7 in aqueous solution: Optimization by Box–Behnken design. *J. Chem. Technol. Biotechnol.* **2021**, *96*, 2647–2658. [CrossRef]
78. El-Sawy, A.M.; Salem, M.A.; Salem, I.A.; Hydara, M.M.; Zaki, A.B. Sonophotocatalytic degradation of malachite green in aqueous solution using six competitive metal oxides as a benchmark. *Photochem. Photobiol. Sci.* **2023**, *22*, 579–594. [CrossRef]
79. Patidar, R.; Srivastava, V.C. Mechanistic and kinetic insights of synergistic mineralization of ofloxacin using a sono-photo hybrid process. *Chem. Eng. J.* **2021**, *403*, 125736. [CrossRef]

Disclaimer/Publisher's Note: The statements, opinions and data contained in all publications are solely those of the individual author(s) and contributor(s) and not of MDPI and/or the editor(s). MDPI and/or the editor(s) disclaim responsibility for any injury to people or property resulting from any ideas, methods, instructions or products referred to in the content.